

Published in final edited form as:

*Anal Chim Acta*. 2012 August 13; 738: 69–75. doi:10.1016/j.aca.2012.06.002.

## Breath acetone monitoring by portable Si:WO<sub>3</sub> gas sensors

Marco Righettoni<sup>a</sup>, Antonio Tricoli<sup>a</sup>, Samuel Gass<sup>a</sup>, Alex Schmid<sup>b,c</sup>, Anton Amann<sup>b,c</sup>, and Sotiris E. Pratsinis<sup>a,\*</sup>

<sup>a</sup>Particle Technology Laboratory, Department of Mechanical and Process Engineering ETH Zurich, CH-8092 Zurich, Switzerland <sup>b</sup>Univ.-Clinic for Anesthesia, Innsbruck Medical University, A-6020 Innsbruck, Austria <sup>c</sup>Breath Research Institute of the Austrian Academy of Sciences, A-6850 Dornbirn, Austria

### Abstract

Breath analysis has the potential for early stage detection and monitoring of illnesses to drastically reduce the corresponding medical diagnostic costs and improve the quality of life of patients suffering from chronic illnesses. In particular, the detection of acetone in the human breath is promising for non-invasive diagnosis and painless monitoring of diabetes (no finger pricking). Here, a portable acetone sensor consisting of flame-deposited and in situ annealed, Si-doped epsilon-WO<sub>3</sub> nanostructured films was developed. The chamber volume was miniaturized while reaction-limited and transport-limited gas flow rates were identified and sensing temperatures were optimized resulting in a low detection limit of acetone (~20 ppb) with short response (10–15 s) and recovery times (35–70 s). Furthermore, the sensor signal (response) was robust against variations of the exhaled breath flow rate facilitating application of these sensors at realistic relative humidities (80–90%) as in the human breath. The acetone content in the breath of test persons was monitored continuously and compared to that of state-of-the-art proton transfer reaction mass spectrometry (PTR-MS). Such portable devices can accurately track breath acetone concentration to become an alternative to more elaborate breath analysis techniques.

### Keywords

Biosensor; Chemo-resistive gas sensor; Metal oxide; Flame spray pyrolysis; Nanoparticles; Cross-sensitivity to humidity

## 1. Introduction

Noninvasive detection of diseases by breath analysis is a fast, economically viable and simple alternative to blood analysis and endoscopy [1]. The breath, however, contains several hundred volatile organic compounds (VOC) with concentrations ranging from ppt to ppm [2]. The cellular and biochemical origin of many of these VOCs has not been determined and some of them might be of exogenous origin [3]. So the field of exhaled breath analysis is still in its infancy. Exceptions are isoprene and acetone, which appear in relatively high concentrations of ~100 and ~500 ppb, respectively [4]. Acetone has the potential of supplementing information on the status of patients suffering from diabetes [5]. The acetone concentration in the breath varies from 300 to 900 ppb in healthy people [4] to more than 1800 ppb for diabetics [6]. Nevertheless, acetone concentrations in the breath are

not simply related to glucose levels in the blood and additional research is necessary to make it a viable marker compound for clinical routine. For example, exchange of acetone between blood and breath is taking place not only in the alveoli but also in the upper airways [7].

Even though the broad application of breath analysis is still challenging, the development of small, hand-held devices for reliable and continuous, real-time measurement of important breath markers such as acetone is desirable. Several methods have demonstrated a remarkable potential for such measurements [8]. For example, gas chromatography with flame ionization detection (FID) [9], proton transfer reaction-mass spectrometry (PTR-MS) [10] selected ion flow tube-mass spectrometry (SIFT-MS) [11], and differential mobility spectroscopy (DMS) [12] have shown high selectivity, sufficient sensitivity and low limit of detection for several VOCs. In general, however, most of these methods are quite costly and have rather limited portability except for DMS that has also high potential for miniaturization [13]. In this regard, chemo-resistive gas sensors based on semiconductor nanoparticles are attractive for breath analysis [14] offering low fabrication costs, high sensitivity, sufficiently low limit of detection and further miniaturization potential [15].

Recently, Cr- or Si-doped  $\text{WO}_3$  nanoparticles have shown high sensitivity and selectivity to acetone [16], even up to 90% relative humidity [17]. This has allowed detection of low concentrations of acetone (down to 20 ppb) with high signal to noise ratio and high selectivity to ethanol and water vapor [17]. These promising results, however, were obtained in large heated chambers and simulated breath conditions. The application of such nanoparticles as acetone detectors in portable devices is not trivial [18] as reaching sufficiently high temperatures (300–450 °C) at reasonable power consumption requires a locally heated substrate that may result in inhomogeneous temperatures and concentration profiles within the sensing film [19]. Thus, the development of a portable device for breath acetone detection is still challenging [8] but quite attractive.

Here, a portable, chemo-resistive sensor has been developed and applied to real breath acetone detection. The sensor was based on a back-heated substrate with a sensing film consisting of optimally performing 10 mol% Si-doped  $\text{WO}_3$  nanoparticles [17]. The sensitivity and selectivity of this device to acetone was investigated at various concentrations, temperatures, relative humidities and gas flow rates. Using this device, the breath acetone concentration of test persons at rest or during physical activity was measured and compared to that measured by highly accurate PTR-MS.

## 2. Materials and methods

A flame spray pyrolysis (FSP) reactor was used for synthesis and direct deposition of 10 mol % Si-doped  $\text{WO}_3$  nanoparticle films [20] onto  $\text{Al}_2\text{O}_3$  substrates featuring a set of interdigitated electrodes (Fig. 1a). A solution of ammonium (meta)tungstate hydrate (Aldrich, purity > 97%) and hexamethyldisiloxane (HMDSO, Aldrich, purity >99%) was created as dictated by the final  $\text{SiO}_2$  content (10 mol%), and diluted in a 1:1 (volume ratio) mixture of diethylene glycol monobutyl ether (Fluka, purity > 98.5%) and ethanol (Fluka, purity > 99.5%) with a total metal (Si and W) concentration of 0.2 M [20]. This solution was supplied at a rate of 5 mL  $\text{min}^{-1}$  through the FSP nozzle and dispersed to a fine spray with 5 L  $\text{min}^{-1}$  oxygen (pressure drop 1.5 bar). That spray was ignited by a supporting ring-shaped premixed methane/oxygen flame ( $\text{CH}_4 = 1.25 \text{ L min}^{-1}$ ,  $\text{O}_2 = 3.2 \text{ L min}^{-1}$ ). An additional 5 L  $\text{min}^{-1}$  sheath oxygen was supplied from an annulus surrounding that flame to ensure excess oxidant flow [20]. The nanoparticles collected downstream of the sensor substrate consisted of pure  $\text{e-WO}_3$  with crystal size of about 10 nm [20]. This nanoparticle film composition was selected for its optimal thermal stability, selectivity and sensitivity even in humid conditions [17]. The alumina substrate (0.8 mm thick) had interdigitated Pt lines

(sputtered, 350  $\mu\text{m}$  width and spacing) and a Pt resistance temperature detector (RTD) on one side and a Pt heater on the other side. The overall dimensions of the alumina substrate were 15 mm  $\times$  13 mm (Electronic Design Center, Case Western Reserve University, Cleveland, OH, USA).

The  $\text{WO}_3$  crystal size and phase composition were characterized by X-ray diffraction (XRD). Prior to sensing tests, the sensors (Fig. 1a) were kept in an oven (Carbolite GmbH, Ubstadt-Weiher, Germany) at 500  $^\circ\text{C}$  for 5 h at ambient pressure to stabilize the nanoparticle size and avoid further sintering during sensor measurements. The simulated breath was prepared by mixing synthetic air (Pan Gas, 99.999%) and humid air (at 20  $^\circ\text{C}$ ) with acetone or ethanol (10 ppm in synthetic air, Pan Gas 5.0) to obtain the desired concentration, as described in more detail elsewhere [17]. To attain lower flow rates ( $<0.2 \text{ L min}^{-1}$ ), a supplementary mass flow controller and a pressure release valve were added. The sensors were placed inside a T-shaped tube chamber, 50 mm in height, 75 mm in length and 18 mm in diameter (Fig. 1a) and placed onto a Macor holder connected to a voltmeter (Keithley, 2700 Multimeter/Data acquisition system) to measure film resistance and to a power source (Hopesun, DC power supply) to heat the sensors. The operating temperature ( $T_0$ ) was varied between 250 and 390  $^\circ\text{C}$  and measured with the embedded Pt RTD on the substrate. Additionally the chamber temperature was measured by a thermocouple (n-type) placed about 15 mm away from the sensor. The chamber temperature increases at the beginning and then stabilizes to a constant value following always that by the Pt RTD. For example, at 350  $^\circ\text{C}$  (RTD) at steady state and at 1  $\text{L min}^{-1}$  inlet gas flow rate, the chamber temperature was about 60  $^\circ\text{C}$ .

The sensor response ( $S$ ) is:  $S = R_{\text{air}}/R_{\text{analyte}} - 1$  where  $R_{\text{air}}$  is the film resistance in air at a given relative humidity (RH) and  $R_{\text{analyte}}$  is that resistance at a given concentration of analyte (acetone, ethanol or water vapor). The cross-sensitivity to humidity (CS) is [21]:  $\text{CS} = \text{abs}[(S_{\text{dry}} - S_{\text{RH}})/S_{\text{dry}}] \times 100$  where  $S_{\text{dry}}$  and  $S_{\text{RH}}$  are the sensor responses in dry air and at a given RH, respectively, as defined earlier [17]. The sensor response time is the time needed to reach 90% of the sensor response to 100 ppb acetone. The recovery time is the time to recover 90% of the sensor response to that of 600 ppb acetone [17].

Real breath measurements (Fig. 1b) were performed with the aid of a respiratory flow controlled mask (Cortex Biophysik GmbH, Leipzig, Germany) that allowed sampling of specific breath segments into the Si:WO<sub>3</sub> sensors and a high-sensitivity PTR-MS (Ionicon Analytik GmbH, Innsbruck) [22]. Gas sampling was accomplished by a heated Teflon tube using an insulated heating wire (TNI Medical, Freiburg, Germany). More precisely, the temperature was kept above 40  $^\circ\text{C}$  along the entire tube length, to minimize any water condensation. A constant flow rate of 70  $\text{mL min}^{-1}$  was kept during all breath measurements while the RTD temperature of the Si:WO<sub>3</sub> sensor was set at 350  $^\circ\text{C}$ . The calibration lines for the Si:WO<sub>3</sub> sensors have been calculated by linear regression from the sensor response of acetone at 90% RH with 70  $\text{mL min}^{-1}$  inlet flow rate. The overall goodness of fit ( $R^2$ ) was above 0.97 indicating high accuracy. Measurements during physical activity are carried out on a computer-controlled, semi-supine medical ergometer (eBikeL, GE Medical Systems, Milwaukee, USA) operating at constant levels of power independently of the pedal speed. A supporting bed stabilizes the torso of the volunteer thereby reducing movement artifacts appearing in the acquired physiological signals. Five male persons (subjects) in good health between 25 and 35 years old were tested. The acetone and isoprene signals were the counts per second measured at mass-to-charge ratio  $m/z = 59$  and 69, respectively. The response time calculated during human breath measurements is defined as the time needed to reach 90% of the final average acetone concentration.

### 3. Results and discussion

#### 3.1. Device characterization

Fig. 1a shows a schematic of the device consisting of a back-heated substrate with a sensing film of silica-doped  $\text{WO}_3$  nanoparticles and a T-shaped chamber. The baseline resistance of the sensors in dry air was investigated as a function of operating temperature. Their baseline was within ca. 2 M $\Omega$  variation for all temperatures, consistent with the expected variability of chemoresistive gas sensors [23]. The average baseline decreased from 22.5 to 1.3 M $\Omega$  by increasing the operating temperature from 150 to 390 °C. The baseline of the present device at 350 °C was about 3 M $\Omega$ : more than 300 times lower than the that of  $\text{SnO}_2$ -based microhotplate sensors operated at even higher temperatures (450 °C) [18] favoring, thus, their integration in monolithic sensing devices [24], where typical target baselines are below 1 G $\Omega$ .

With respect to acetone sensing, both the catalytic activity of the semiconductor  $\text{WO}_3$  surface and its electrical properties are strongly influenced by temperature [25]. The sensor response to 500 ppb acetone (circles) and ethanol (diamonds) was investigated as function of film temperature (Fig. 2a). The maximum response to acetone was at 350 °C, requiring about 9 W to heat up the substrate. The observed reduction in sensor response at temperatures above this optimum was attributed to the increased combustion of acetone in the upper layers of the sensing film [26], reducing the acetone amount penetrating to lower layers. At 350 °C, the response of the back-heated sensor was comparable to that in heated chambers [17] at 400 °C. This is advantageous as lower operating temperatures require less power improving the portability and lowering the energy needs of the device [27].

The average ethanol concentration in the breath [28] is approximately 196 ppb with a standard deviation of 224 ppb, making it a potentially disturbing analyte during breath acetone measurement. Here, the sensor response to 500 ppb ethanol (Fig. 2a) was considerably lower than that to 500 ppb acetone at all temperatures demonstrating good acetone selectivity. Furthermore, the maximal response to ethanol was at slightly lower temperatures (325 °C) than for acetone. This difference in optimum sensing temperature between acetone and ethanol increased the acetone selectivity towards ethanol from 6.9 at 300 °C to 13.4 when operating the detector at 350 °C.

Fig. 2b shows the sensor response to acetone (circles) and ethanol (diamonds) as a function of their concentration at 350 °C. The acetone sensor response (Fig. 2b, circles) was always 9–13 times higher than that of ethanol (diamonds), resulting in considerably higher acetone selectivity here than that (4.7–6.7) within the heated chamber [17]. This difference is attributed to the different operating temperature and chamber geometry. Furthermore, the operating temperature in heated chambers was above the autoignition temperature of ethanol (365 °C) that could have led to its partial decomposition to more reactive species, yielding a higher response. Allowing a maximal measurement error of the acetone concentration (500–1500 ppb) of 5%, the sensor response ratio between acetone and the average breath ethanol concentration (196 ppb) must be above 20. For example, at the lowest limit of 500 ppb acetone concentration, the sensor response is 1.54 (Fig. 2b) while that of ethanol at 196 ppb is about 0.06 (Fig. 2b) resulting in a sensor response ratio of 25.6. The error bars on the acetone sensor response (Fig. 2b, circles) show the variability of different sensors.

The gas flow rate over the sensing film might be another challenge as its variation may affect the sensor output [29] if a reaction-limited response is not reached [26]. Design of devices with sufficiently high flow velocity can be achieved in line with a diffusion-reaction model [26] for chemo-resistive gas sensors. Here, variation in the gas flow rate from 0.05 (Fig. 3, crosses) to 1 L min<sup>-1</sup> (circles) has been investigated. For a gas to be detected, it

needs first to diffuse into the sensing film and react on the metal oxide surface. For sufficiently high analyte flux into the sensing film, a reaction-limited response is reached that is mainly a function of film temperature, morphology and material properties. If the analyte flux, however, is not sufficient, a transport (diffusion)-limited sensor response is obtained. Flow rates between 0.2 and 1 L min<sup>-1</sup> (Fig. 3, black lines), corresponding to flow velocities of 0.015 and 0.08 m s<sup>-1</sup> respectively, supplied to the present back-heated sensors, resulted in sufficiently high analyte mass flux to reach a reaction-limited response: this results in almost identical sensor responses (<4% difference). By decreasing, however, the flow rate substantially below 0.2 L min<sup>-1</sup> (grey lines) yields a flow rate dependency similar to that in heated chambers [29] indicating a transport (diffusion)-limited response. The sensor response is reduced by about 15% when decreasing the flow rate from 0.2 (black squares) to 0.1 L min<sup>-1</sup> (grey diamonds) and decreases continuously with lower flow. Flow rates higher than 0.2 L min<sup>-1</sup> (reaction-limited) are more relevant to breath analysis as average expiratory flow rates of healthy persons are above 2.4 L min<sup>-1</sup> [30]. However, state-of-the-art measurement devices such as PTR-MS utilize lower (e.g. 70 mL min<sup>-1</sup>) flow rates. Here the latter were used for the Si:WO<sub>3</sub> sensors to facilitate their comparison to established PTR-MS.

The present sensor response to water vapor from 10 to 90% RH was minimal (<0.3) in agreement with results obtained in externally heated chambers [17]. Despite this high selectivity against H<sub>2</sub>O, it must be noted that the water vapor content of the inlet flow reduced considerably the temperature of the sensor, so its power supply needs to be slightly adjusted to maintain the same sensor temperature (350 °C).

Fig. 4a shows the cross sensitivity (CS) to humidity as a function of acetone concentration for RH ranging from 0 to 90%. The most significant reduction in sensor response was observed when increasing the RH from 0 to 20%, a rather unrealistic RH range for breath analysis. Beyond this point, the CS to humidity decreased considerably. So, the CS was 54% between 0 and 90% RH but only 4.5% between 80 and 90% RH. This indicates that the acetone concentration in the breath could be determined using this sensor with sufficient accuracy even without additional RH measurement. Furthermore, the sensor response to the water content of the breath (90% RH) from the background ambient condition (40% RH) is less than 0.03 (with  $S = R_{40\%RH}/R_{90\%RH} - 1$ , where  $R_{40\%RH} = 2.43 \pm 0.03 \text{ M}\Omega$  and  $R_{90\%RH} = 2.43 \pm 0.02 \text{ M}\Omega$ ), which is within the sensor baseline variability and rather small compared to acetone response: about 1.85 for 600 ppb acetone for 1 L min<sup>-1</sup> (Fig. 3).

A patient's exhalation time is limited by his or her forced vital capacity (FVC) and expiratory flow, both of which vary considerably depending on age, sex, and health [31]. As a result, small response and recovery times facilitate the application of the device in breath analysis. Fig. 4b shows the response (open circles) and recovery (filled circles) times of these Si:WO<sub>3</sub> sensors as a function of RH at 350 °C. The response time was not affected by variations in RH from 0 to 90% and remained constant to ca. 14 s. In contrast, the recovery time (filled circles), increased from 36 to 62 s in that RH range. These response times were 5 to 25 times smaller than those in heated chambers [17]. This is attributed to two effects: (1) heated chambers are characterized by large volumes of almost stagnant fluid and peripheral position of the sensor and thus the response time is more a measurement of the transient concentration within the chamber rather than a characteristic feature of the device [19]. (2) Due to rapid inlet velocity of the impinging jet and resulting turbulence here, the analyte mass flux to the sensing film of the present device was considerably higher. While it might be possible to achieve faster measurements by improving the electronics [32], the present device already has sufficiently short response time to acetone.

Fig. 5 shows a clear reduction of sensor resistance from 2.51 to 2.41 M $\Omega$  in response to even 20 ppb acetone at 90% RH corresponding to a sensor response of 0.042 which is comparable to that (0.08) in bulkier, heated chambers at 400 °C [17]. Furthermore, this sensor exhibited a high signal to noise ratio (>10) and the ability to differentiate in sensor response (10%) even between 50 ppb and 60 ppb of acetone, further indicating the accuracy of the present sensor and that even lower limits of detection are possible.

### 3.2. Exhaled breath analysis

Undoubtedly, real breath measurements are needed to validate the present devices for breath acetone monitoring. Here, human breath was analyzed simultaneously by this novel sensor device and by state-of-the-art, high-sensitivity PTR-MS. As the alveolar levels of blood-borne volatile species, such as acetone and isoprene, are best reflected by the end tidal fraction of each exhalation phase [33], here, the end tidal volume of the breath was sampled by a flow-controlled valve (Fig. 1b).

Fig. 6a shows the concentration of acetone in tidal part of the respiratory cycle of a healthy test person at rest measured by the present Si:WO<sub>3</sub> sensor (thick solid line) and PTR-MS for acetone (thin solid line) and isoprene (dotted line). The acetone concentration measured by Si:WO<sub>3</sub> sensor was calculated from the calibrated sensor response at 90% RH and at 70 mL min<sup>-1</sup> flow. At the start of breath sampling (~3 min), the sensor resistance decreased rapidly and recovered to the initial value after stopping the breath flow (~8 min). The calibrated sensor response corresponded to about 970 ppb acetone concentration on the average at 3–8 min. This was in good agreement (>98%) with the acetone concentration reading of the PTR-MS, 980 ppb (thin solid line). The present Si:WO<sub>3</sub> sensor measured a similar acetone concentration evolution as the PTR-MS and even had a higher signal to noise ratio (60 and 9, respectively).

The visible drift for the acetone sensor response (Fig. 6a, thick solid line) is probably due to a catalytic surface reaction of other species present in the breath (e.g. CO) that locally increase the temperature causing also the initial overshoot of the Si:WO<sub>3</sub> response. This leads to an initial drop in the resistance that later stabilizes toward that corresponding predominantly to acetone. This has been previously observed by Pt-doped SnO<sub>2</sub> sensors during CO detection [18]. A comparable but smaller drift is also visible for the average PTR-MS signal. The response time to human breath (Fig. 6a), was of 27 and 28 s for the Si:WO<sub>3</sub> sensor and PTR-MS, respectively. This is comparable but longer than that measured for simulated breath condition (Fig. 4b, open circles). As expected, the isoprene concentration measured by PTR-MS (dotted line) remained rather constant during normal breathing without physical activity (Fig. 6a).

The acetone breath concentration measured from the same person during the same day by the Si:WO<sub>3</sub> sensor did not change much during physical activity (Fig. 6b, thick solid line) compared to that in Fig. 6a in agreement also with the acetone concentration measured here by PTR-MS (thin solid line). A similar overshoot in the acetone concentration measured by the Si:WO<sub>3</sub> sensor is visible as discussed above and its average concentration was about 970 ppb, as in Fig. 6a (thick solid line). In contrast, the concentration of isoprene, measured by PTR-MS (Fig. 6b) increased from about 100 to above 240 ppb in agreement with the reported release of isoprene during physical activity [33]. The acetone concentration measured by the Si:WO<sub>3</sub> sensor (Fig. 6b, thick solid line) followed again the acetone concentration evolution by PTR-MS (thin solid line) and was hardly affected by the presence of isoprene. The alveolar ventilation increased from about 10 to 20 L min<sup>-1</sup> at the start of the physical activity and decreased back to 10 L min<sup>-1</sup> at its end. These results show that the present Si:WO<sub>3</sub> sensors are quite robust against changes in ventilation rate and in the presence of isoprene. Furthermore, these sensors were in agreement with PTR-MS for

acetone concentrations (ranging from 590 to 980 ppb) from different healthy test persons (for 4–6 min). The sensor was able to detect differences in breath acetone concentrations from 880 to 980 ppb. Nevertheless, testing the breath in the morning after breakfast with lower acetone (~600 ppb) concentrations resulted in an inferior (~85%) but still comparable agreement between this sensor and PTR-MS.

The response of the Si:WO<sub>3</sub> sensors was also tested to short breath pulses (Fig. 7), without controlling valve, as may be necessary in applied breath analysis. The sensors had response times of about 10 s and thus were able to fully capture the pulse profile. The sensor response to breath pulses (Fig. 7) of each test person were fairly reproducible and sensitive to even small acetone concentration changes, always recovering the initial baseline for each test person. Test person 3, for instance, showed higher sensor response than that of the two other test persons indicating higher acetone concentration in the breath. However, due to different transient time (e.g. sampling flow rate) it was not possible to compare it directly with PTR-MS measurements.

## 4. Conclusions

Portable acetone sensors made of 10 mol% Si-doped WO<sub>3</sub> nanoparticles were developed and tested for breath analysis. They demonstrated a strong potential for detection of acetone, a breath marker for diabetes, both in ideal (dry air) and realistic conditions (90% RH). The sensors were highly selective over ethanol and sensitive to acetone, regardless of background RH. The sensor response times were below 15 s at application typical conditions, making these devices attractive for breath analysis. Acetone concentrations as low as 20 ppb were measured with high signal to noise ratios (>10). Furthermore, the sensor signal (response) was robust against variation in gas (or breath) flow rates down to 0.2 L min<sup>-1</sup> facilitating application of such sensors in real breath measurement conditions.

These sensors were applied to breath acetone monitoring of five different test persons and were in agreement (>98%) to high-sensitivity PTR-MS measurements of the same breath samples. The breath acetone concentrations measured by the Si:WO<sub>3</sub> sensors had very high signal to noise ratio (60) and the response time was about 27 s. The Si:WO<sub>3</sub> sensors were selective to acetone both at rest and during physical activity, independently of the respiratory pace or presence of isoprene that is associated with physical activity. Furthermore, these sensors also responded very rapidly to short breath pulses further supporting their potential for breath analysis.

## Acknowledgments

This research was supported by the Swiss National Science Foundation, grant 200021\_130582/1 and the European Research Council. The authors are grateful to J. King (BRI, Austria) for his assistance during the breath analysis experiments.

## References

- [1]. Amann A, Corradi M, Mazzone P, Mutti A. *Expert. Rev. Mol. Diagn.* 2011; 11:207–217. [PubMed: 21405971]
- [2]. Phillips M, Gleeson K, Hughes JMB, Greenberg J, Cataneo RN, Baker L, McVay WP. *Lancet.* 1999; 353:1930–1933. [PubMed: 10371572]
- [3]. Filipiak W, Sponring A, Filipiak A, Ager C, Schubert J, Miekisch W, Amann A, Troppmair J. *Cancer Epidemiol. Biomarkers Prev.* 2010; 19:182–195. [PubMed: 20056637]
- [4]. Diskin AM, Spanel P, Smith D. *Physiol. Meas.* 2003; 24:107–119. [PubMed: 12636190]
- [5]. Ping W, Yi T, Xie HB, Shen FR. *Biosens. Bioelectron.* 1997; 12:1031–1036. [PubMed: 9451791]
- [6]. Deng CH, Zhang J, Yu XF, Zhang W, Zhang XM. *J. Chromatogr. B.* 2004; 810:269–275.

- [7]. King J, Unterkofler K, Teschl G, Teschl S, Koc H, Hinterhuber H, Amann A. *J. Math. Biol.* 2011; 63:959–999. [PubMed: 21234569]
- [8]. Risby TH, Solga SF. *Appl. Phys. B.* 2006; 85:421–426.
- [9]. Sanchez JM, Sacks RD. *Anal. Chem.* 2003; 75:2231–2236. [PubMed: 12918960]
- [10]. Schwarz K, Filipiak W, Amann A. *J. Breath Res.* 2009; 3:027002. [PubMed: 21383457]
- [11]. Smith D, Spanel P. *Mass Spectrom. Rev.* 2005; 24:661–700. [PubMed: 15495143]
- [12]. Shnayderman M, Mansfield B, Yip P, Clark HA, Krebs MD, Cohen SJ, Zeskind JE, Ryan ET, Dorkin HL, Callahan MV, Stair TO, Gelfand JA, Gill CJ, Hitt B, Davis CE. *Anal. Chem.* 2005; 77:5930–5937. [PubMed: 16159124]
- [13]. Davis CE, Bogan MJ, Sankaran S, Molina MA, Loyola BR, Zhao W, Benner WH, Schivo M, Farquar GR, Kenyon NJ, Frank M. *IEEE Sens. J.* 2010; 10:114–122.
- [14]. Fleischer M, Simon E, Rumpel E, Ulmer H, Harbeck M, Wandel M, Fietzek C, Weimar U, Meixner H. *Sens. Actuator B: Chem.* 2002; 83:245–249.
- [15]. Tricoli A, Righettoni M, Teleki A. *Angew. Chem. Int. Ed.* 2010; 49:7632–7659.
- [16]. Wang L, Teleki A, Pratsinis SE, Gouma PI. *Chem. Mater.* 2008; 20:4794–4796.
- [17]. Righettoni M, Tricoli A, Pratsinis SE. *Anal. Chem.* 2010; 82:3581–3587. [PubMed: 20380475]
- [18]. Tricoli A, Graf M, Mayer F, Kuhne S, Hierlemann A, Pratsinis SE. *Adv. Mater.* 2008; 20:3005–3010.
- [19]. Lezzi AM, Beretta GP, Comini E, Faglia G, Galli G, Sberveglieri G. *Sens. Actuator B: Chem.* 2001; 78:144–150.
- [20]. Righettoni M, Tricoli A, Pratsinis SE. *Chem. Mater.* 2010; 22:3152–3157.
- [21]. Tricoli A, Righettoni M, Pratsinis SE. *Nanotechnology.* 2009; 20:315502. [PubMed: 19597246]
- [22]. Bajtarevic A, Ager C, Pienz M, Klieber M, Schwarz K, Ligor M, Ligor T, Filipiak W, Denz H, Fiegl M, Hilbe W, Weiss W, Lukas P, Jamnig H, Hackl M, Haidenberger A, Buszewski B, Miekisch W, Schubert J, Amann A. *BMC Cancer.* 2009; 9:348. [PubMed: 19788722]
- [23]. Madler L, Roessler A, Pratsinis SE, Sahn T, Gurlo A, Barsan N, Weimar U. *Sens. Actuator B: Chem.* 2006; 114:283–295.
- [24]. Graf M, Frey U, Taschini S, Hierlemann A. *Anal. Chem.* 2006; 78:6801–6808. [PubMed: 17007499]
- [25]. Aguir K, Lemire C, Lollman DBB. *Sens. Actuator B: Chem.* 2002; 84:1–5.
- [26]. Becker T, Ahlers S, Bosch-v.Braunmuhl C, Muller G, Kieseewetter O. *Sens. Actuator B: Chem.* 2001; 77:55–61.
- [27]. Graf M, Barrettino D, Taschini S, Hagleitner C, Hierlemann A, Baltes H. *Anal. Chem.* 2004; 76:4437–4445. [PubMed: 15283585]
- [28]. Turner C, Spanel P, Smith D. *Rapid Commun. Mass Spectrom.* 2006; 20:61–68. [PubMed: 16312013]
- [29]. Righettoni M, Tricoli A. *J. Breath Res.* 2011; 5:037109. [PubMed: 21828897]
- [30]. Mahut B, Delacourt C, Zerah-Lancner F, De Blic J, Harf A, Delclaux C. *Chest.* 2004; 125:1012–1018. [PubMed: 15006962]
- [31]. Schoenberg JB, Beck GJ, Bouhuys A. *Respir. Physiol.* 1978; 33:367–393. [PubMed: 705072]
- [32]. Baraton MI. *Sens. Actuator B: Chem.* 1996; 31:33–38.
- [33]. King J, Kupferthaler A, Unterkofler K, Koc H, Teschl S, Teschl G, Miekisch W, Schubert J, Hinterhuber H, Amann A. *J. Breath Res.* 2009; 3:027006. [PubMed: 21383461]



**HIGHLIGHTS**

- ▶ Portable sensors were developed and tested for monitoring acetone in the human breath.
- ▶ Acetone concentrations down to 20 ppb were measured with short response times (<30 s).
- ▶ The present sensors were highly selective to acetone over ethanol and water.
- ▶ Sensors were applied to human breath: good agreement with highly sensitive PTR-MS.
- ▶ Tests with people at rest and during physical activity showed the sensor robustness.

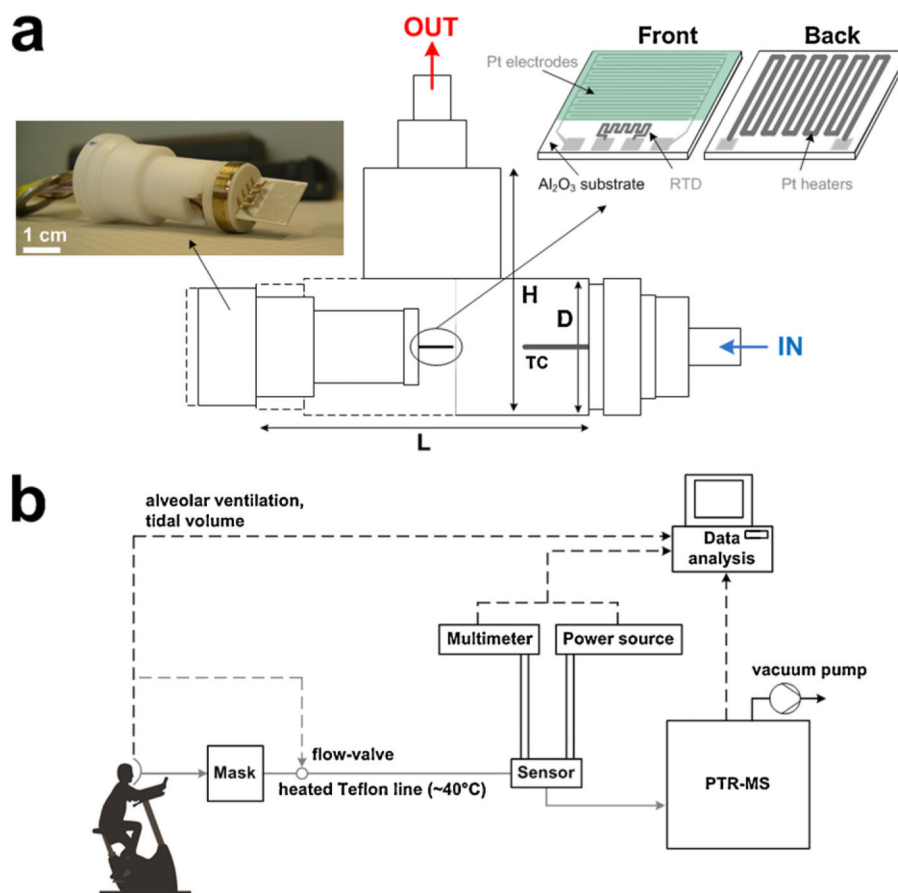


**Fig. 1.** Schematic of the T-shaped chamber ( $L = 75$ ,  $H = 50$  and  $D = 18$  mm) and thermocouple (TC) placed inside. A Macor piece is holding the sensor prior to deposition of a tungsten oxide ( $\text{WO}_3$ ) film onto interdigitated Pt electrodes laid on an  $\text{Al}_2\text{O}_3$  substrate along with a resistance temperature detector (RTD) on the front side and a Pt heater on its back. (b) Schematic of the experimental set-up during breath analysis. The breath flow (grey lines) is controlled by the mask and kept constant by the PTR-MS pump. All the data (dashed lines) are collected and analyzed by the computer.

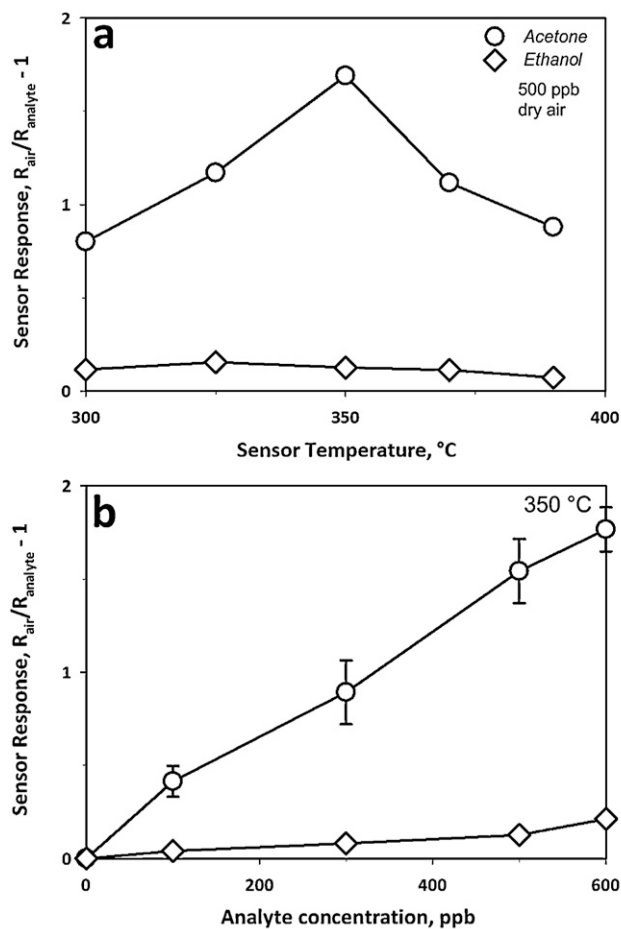


**Fig. 2.** Sensor response (a) to 500 ppb acetone (circles) or ethanol (diamonds) as a function of sensor temperature in dry air, with an optimum at 350 °C; and (b) to different acetone (circles) and ethanol (diamonds) concentrations at 350 °C. The error bars represent the variability of sensor response to acetone (circles) by three 10 mol% Si-doped  $\text{WO}_3$  sensors.

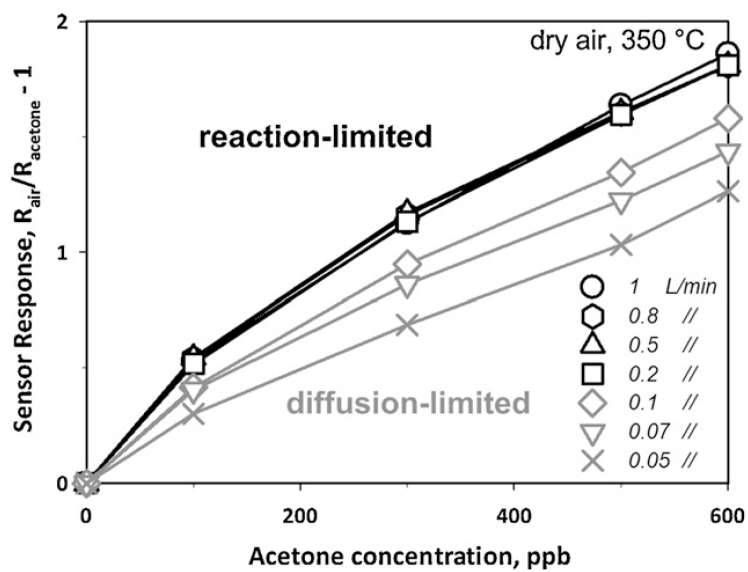


**Fig. 3.** Sensor response to acetone concentration as a function of inlet total gas flow rate (from 0.05 to 1 L min<sup>-1</sup>). The sensor response is constant above 0.2 L min<sup>-1</sup> (black symbols) as it is reaction-limited. Below that the sensor response becomes transport (diffusion)-limited and decreases with decreasing inlet gas flow rate (grey symbols).

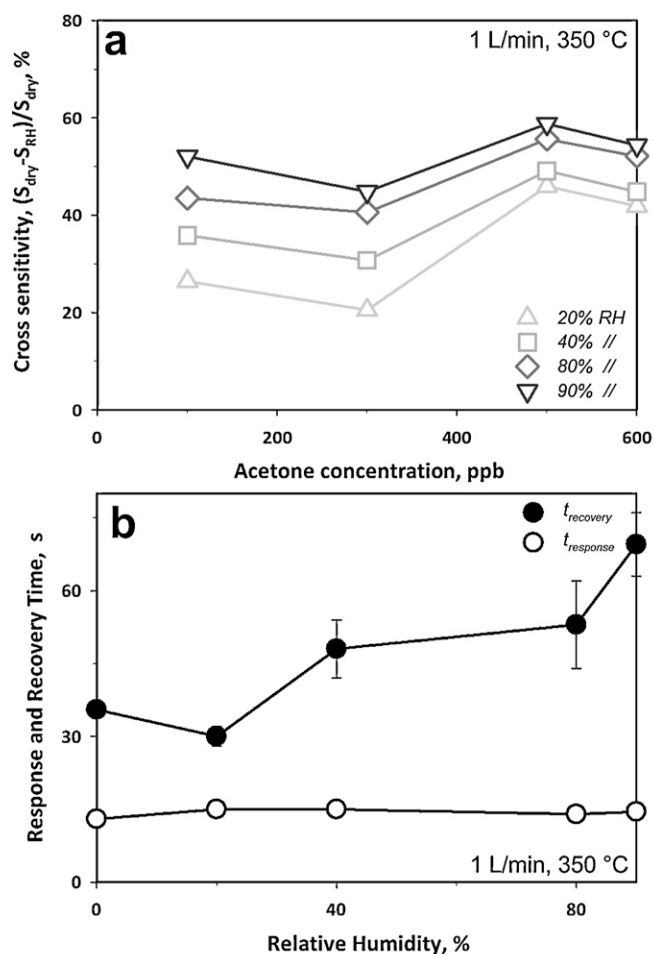


**Fig. 4.** (a) Sensor response upon exposure to increasing acetone concentration at various RH. The sensor response to acetone decreased with increasing RH showing high CS (54%) between 0 and 90% RH. Between 80 and 90% RH, however, the CS was only 4.5% showing the robustness of such sensors at the typical RH of the human breath. (b) Response time to 100 ppb (open circles) and recovery time to 600 ppb (filled circles) acetone as a function of RH at 350 °C.

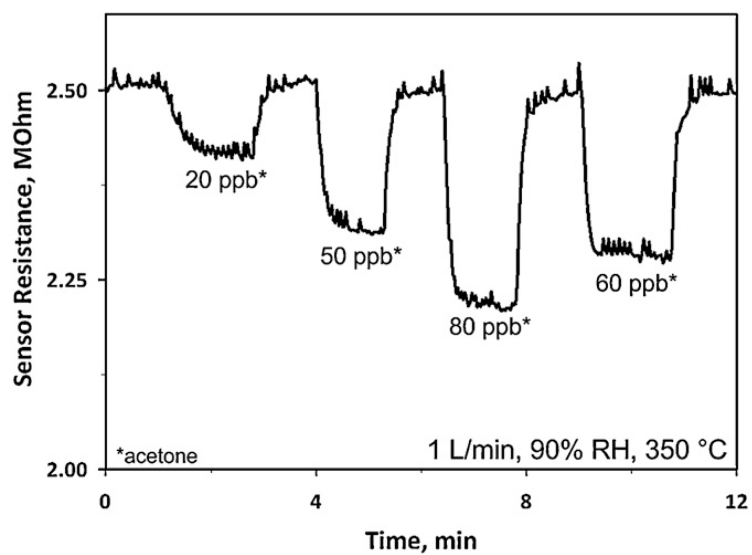


**Fig. 5.** Sensor resistance at 90% RH and upon exposure to ultra low concentrations of acetone (20, 50, 60 and 80 ppb) at 350 °C. The signal noise arises from small temperature fluctuations.

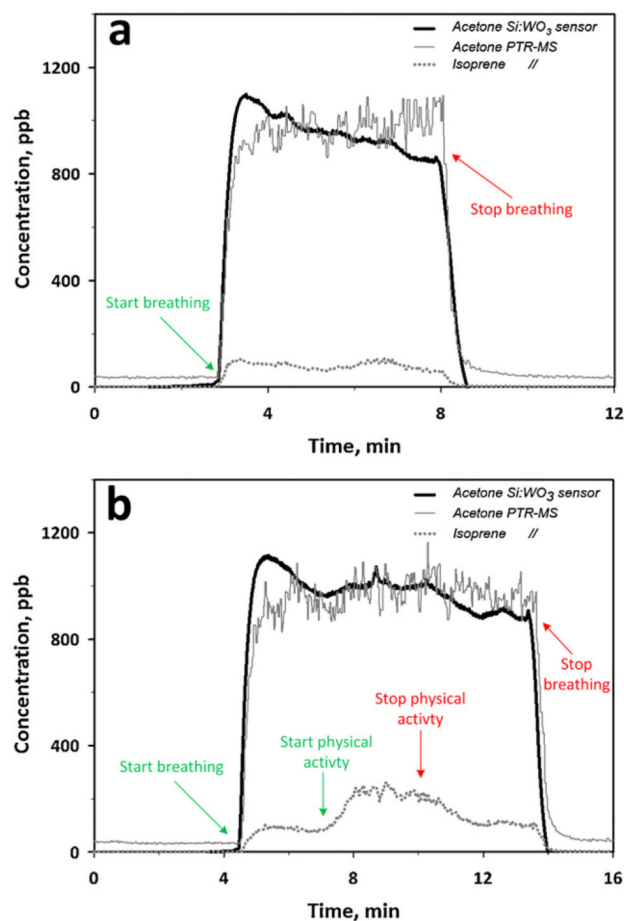


**Fig. 6.** Expected acetone concentration by the Si:WO<sub>3</sub> sensor (thick solid line) and acetone (thin solid line) and isoprene (dotted line) concentrations measured by PTR-MS during breathing of a test person (a) at rest and (b) during physical activity. Even though the isoprene concentration (dotted line) varied notably during physical activity, it does not influence the Si:WO<sub>3</sub> sensor response indicating that its acetone signal is quite robust and selective.

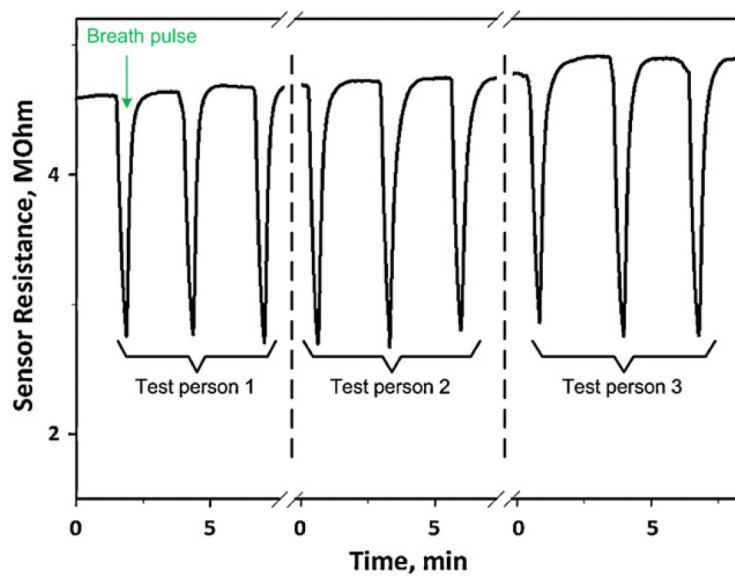


**Fig. 7.** Si:WO<sub>3</sub> sensor response to short pulses of three different healthy test persons with similar breath acetone concentrations.